THE ASTROPHYSICAL JOURNAL, 498:L107–L110, 1998 May 10

DETAILED MASS MAP OF CL 0024+1654 FROM STRONG LENSING

J. ANTHONY TYSON, GREG P. KOCHANSKI, AND IAN P. DELL'ANTONIO
Bell Laboratories, Lucent Technologies, 700 Mountain Avenue, Murray Hill, NJ 07974; tyson@bell-labs.com, gpk@bell-labs.com, dellantonio@bell-labs.com
Received 1997 September 12; accepted 1998 January 21; published 1998 April 27

ABSTRACT

We construct a high-resolution mass map of the $z = 0.39$ cluster 0024+1654, based on a parametric inversion of the associated gravitational lens. The lens creates eight well-resolved subimages of a background galaxy, seen in deep imaging with the *Hubble Space Telescope*.[1] Excluding mass concentrations centered on visible galaxies, more than 98% of the remaining mass is represented by a smooth concentration of dark matter centered near the brightest cluster galaxies, with a 35 h^{-1} kpc soft core. The asymmetry in the mass distribution is less than 3% inside 107 h^{-1} kpc radius. The dark matter distribution we observe in CL 0024 is far more smooth, symmetric, and nonsingular than in typical simulated clusters in either $\Omega = 1$ or $\Omega = 0.3$ cold dark matter cosmologies. Integrated to a 107 h^{-1} kpc radius, the rest-frame mass-to-light ratio is $M/L_V = 276 \pm 40\ h\ \ (M/L_V)_\odot$.

Subject headings: cosmology: observations — galaxies: cluster: individual (CL 0024+1654) — galaxies: formation — gravitational lensing — methods: observational

1. INTRODUCTION

The distribution of mass within high-redshift clusters of galaxies can be a powerful test of theories of gravitational clustering and may give clues to the nature of dark matter (Ostriker & Cen 1996; Eke, Cole, & Frenk 1996). High-resolution mass maps of clusters would place constraints on both Ω and the nature of the dark matter (Crone, Evrard, & Richstone 1994, 1996; Mohr et al. 1995) because different scenarios for structure formation predict observably different mass clumping and segregation in clusters. However, previously it has not been possible to map the mass distribution in clusters in sufficient detail to view mergers and galaxy-cluster mass segregation. Neither galaxy light nor hot gas necessarily traces the total mass distribution precisely (see Schindler & Böhringer 1993). Although weak lensing, X-ray, and kinematic studies of clusters of galaxies set useful limits, there has not been a direct observation on scales as small as 1 kpc and $10^9\ M_\odot$ of the mass segregation between individual galaxies and the cluster. Strong lensing of a highly resolved source galaxy can provide the information required for such a reconstruction.

When multiple gravitationally lensed images of a complex source occur, the mass density is strongly constrained because each feature in the source galaxy must be matched in each of the multiple images. We construct this high-resolution map of the mass distribution in CL 0024+1654 by combining a parametric mass model with a parametric source luminosity model and making a detailed match to the *Hubble Space Telescope* (*HST*) image. Qualitative comparisons of this map can be made with existing simulations. Low-density ($\Omega = 0.3$), flat cosmologies, as well as $\Omega = 1$ standard cold dark matter (SCDM), show considerable mass subclustering on 200 h^{-1} kpc scales (Jing, Mo, & Fang 1995) for redshifts $z > 0.2$. Likewise, Frenk et al. (1996) separately follow "galaxies," gas, and dark matter in SCDM simulations and find large, high-contrast lumps of mass surviving to $z = 0.1$ in virtually all cases. By contrast, simulations of open cosmologies ($\Omega = 0.1$, $\Lambda = 0$) have very little substructure, even at redshifts of 0.5 and higher (Jing et al. 1995; Evrard et al. 1993). Simulations will soon have sufficient resolution and dynamic range to allow a quantitative comparison with the data. Thus, detailed mass maps of clusters at $z > 0.3$ can help to distinguish between these scenarios. Here we examine the mass distribution in the central 200 h^{-1} kpc of one such cluster.

2. PARAMETRIC SOURCE AND MASS MODELS

CL 0024+1654 is an optically rich cluster of galaxies at $z = 0.39$ with a velocity dispersion of $\sigma_v = 1200$ km s^{-1} (Dressler & Gunn 1992) and an X-ray luminosity $L_X = (5.0 \pm 0.6) \times 10^{43}\ h^{-2}$ ergs cm^{-2} s^{-1} (Smail et al. 1997). A single background galaxy, easily recognizable because of its color and peculiar morphology, is multiply imaged (see Colley, Tyson, & Turner 1996). After subtracting the light of the cluster galaxies, we find a total of eight subimages of the background galaxy. We parameterize the source as 58 smooth disks of light. Each of these disks is characterized by an intensity, a scale radius, and the (x, y) position on the source plane (four parameters). A source plane resolution of 0.″007 pixel^{-1} was chosen to allow sufficient evaluations of the model to be done within a reasonable time (12 months) and to allow the model to represent almost all details of the observations. The disks are overlapping, with a median FWHM of 0.″062. A further discussion of the morphology of the source galaxy can be found in Tyson, Kochanski, & Dell'Antonio (1997). The light from this source is then ray-traced through the lens plane, and the resulting image is compared on a pixel-by-pixel basis with the *HST* image. In this way, we obtain a statistically meaningful estimate of the goodness of fit.

Because elliptical potentials can be unphysical (Schramm 1994), we parameterize the mass distribution in CL 0024 as a cluster of mass concentrations ("mascons"). Each mascon is based on a power-law (PL) model (Schneider, Ehlers, & Falco 1993, p. 244) for the mass density $\Sigma(r)$ versus projected radius r, with both an inner core radius and an outer cutoff radius:

$$\Sigma(x) = \frac{K_1 (1 + \gamma x^2)}{(1 + x^2)^{2-\gamma}}, \quad x < X_0,$$
$$\Sigma(x) = K_2 x^{-3} X_0^3, \quad x \geq X_0, \tag{1}$$

where $x = r/r_{\rm core}$, $X_0 = r_{\rm cutoff}/r_{\rm core}$, and γ is the PL model index.

[1] Based on observations with the NASA/ESA *Hubble Space Telescope*, obtained at the Space Telescope Science Institute, which is operated by AURA, Inc., under NASA contract NAS 5-26555.

The constants K_2 and K_1 are related by requiring continuity at $x = X_0$. $K_1^{0.5}$ is proportional to the central line-of-sight velocity dispersion. We build up elliptical mass distributions by superposing a line of overlapping circular mascons. In principle, each mascon is described by nine parameters. The first four come directly from the equation above (K_1, an inner mass core radius $r_{\rm core}$, an outer mass cutoff $r_{\rm cutoff}$, and the slope of the mass profile γ). For elliptical mass distributions, there are three parameters describing the ellipticity (the position angle θ, the length of the line of mascons $l_{\rm core}$, and the uniformity of the spacing of the mascons along the line). For mass components not associated with optically observed galaxies, the *x*- and *y*-positions in the lens plane are also free.

The mass and linear scale sensitivity of this parametric lens inversion technique vary with position in the cluster; cluster mascons projected near a long arc have the effect of their mass distribution highly magnified. For galaxies that are more than about 5″ from the arcs, only their total mass matters, and we parameterize this by the cutoff radius (because $M \propto r_{\rm cutoff}$). Galaxies farther than about 20″ from the arcs are parameterized in groups. On average, we have one parameter per galaxy. However, galaxies on the arcs can typically support several free parameters each.

In practice, one or more mascon is assigned to each of the 118 cluster galaxies, with the number of free parameters for each mascon depending on the distance from the arcs. In addition, 25 free mascons were required for the remaining cluster mass. We refer to this as the "dark matter" (DM), even though it also includes the mass of the hot X-ray gas. We will discuss the mass distribution internal to the cluster galaxies elsewhere (Dell'Antonio, Kochanski, & Tyson 1998). Two large, diffuse, mascons contain 98% of the mass not associated with the galaxies. All parameters were free in both.

In all, the mass and source models are determined by 512 parameters. However, we have over 3800 significantly nonzero (3 σ) pixels in the arcs. Because the optical point-spread function of the Wide Field Planetary Camera 2 is smaller than 1 pixel, the signal is nearly uncorrelated, even on neighboring pixels; thus, we have many more independent constraints than model parameters. In addition, pixels with no signal serve as constraints, because they prevent the model from putting flux in areas of the image where it should not. The resulting mass model is overconstrained and is, in this sense, unique. The resolution of the mass model is set by the spacing of the mass components in the parametric model and is everywhere much lower than the formal Nyquist maximum resolution of 2 pixels.

As we developed the model, it had enough power to predict the central image, based on the three major arcs, then to correctly predict the multiple subimages near the outer arcs. We measure the fit by taking boxes (approximately 10″ square) around each of the arc images and creating model images of each arc using the light and mass models. The image and models are then compared pixel by pixel. The χ^2 per degree of freedom is then calculated for each realization and is iteratively optimized (see Kochanski, Tyson, & Dell'Antonio 1998). Error bars were determined by bootstrap resampling (Efron 1982) and simulated annealing. For the former, the weight given to each pixel was varied randomly while allowing the parameters to vary. In the latter case, we allow the optimizer to accept increases in χ^2 with probability exp $(-\Delta\chi^2)$. We ran both with the full set of parameters free and also with subsets of 7–50 parameters (chosen to capture important correlations) free. These observed variations in parameter values determine the errors (given as 1 σ in this Letter) and control how many parameters may be added in a given region; too many parameters for a galaxy create near-degeneracies and locally large errors. Our calculated errors naturally include the effects of correlations between parameters for neighboring mascons. Nearby galaxies can trade mass, but the total tends to be conserved, leading to better accuracy on larger scales.

3. GLOBAL MASS SOLUTION AND SUBSTRUCTURE

The galaxy masses in the model were initialized using the Faber-Jackson relation. When the model evolved to a low χ^2, we performed robustness tests by perturbing the position and/or mass of a mascon and observing the reconvergence to the solution. Over 2×10^6 models were searched to reach the solution. A color rendering of the projected total mass density, including galaxies, is given in Figure 1 (Plate L4). Optically observed galaxies are fitted by small-core PL models and are blue in the figure. In addition to the large diffuse mascons, other mascons were added to our fit to allow it to match the complexity of the cluster's mass distribution. We will discuss the properties of these small "dark" objects in detail elsewhere (Kochanski et al. 1998). Because most of these mascons represent small fluctuations in the mass density, they should generally be regarded not as distinct objects but as a representation of the local asymmetry or substructure in the mass distribution. Indeed, one of the major results of this Letter is that these subsidiary mascons are quite light, and hence the mass distribution is smooth.

The vast majority of the mass is not associated with the galaxies and appears as a smooth elliptical distribution (shown in red in Fig. 1) centered near the position of the brightest galaxy and elongated in the southeast-northwest direction. The elongation is in the same direction as that of the X-ray isophotes. It is fitted by two massive superposed mass distributions (groups of mascons), one with a 34″ core radius and the other with a 18″ core. These major mascons are centered within 2″ of each other. This DM not associated with galaxies shows no evidence of infalling massive clumps: other than these two major clumps, we find no dark mascons with total mass greater than $5 \times 10^{12}\ h^{-1}\ M_\odot$ (1.5% of the cluster mass), out of the 25 in the fit.

Figure 2 (Plate L5) shows a contour plot of this dark mass not associated with galaxies, plotted over the *HST* blue image. Figure 3 (*top panel*; Plate L6) shows a color image of this diffuse DM, with the model arcs superposed for reference. The inner arc (*E*) may be seen near the center. The bottom panel of Figure 3 shows the diffuse light component smoothed with a 0.″3 Gaussian, with the *HST* images of the arcs superposed in color for reference. The DM has a soft core and is not consistent with the singular mass density profiles found in cold dark matter (CDM) simulations (Moore et al. 1997; Thomas et al. 1997). We have quantified the strongest allowable singularity in terms of adding an additional compact mascon into the fit. We sampled 20 locations for an extra mascon in the central 30 kpc, which would correspond to the difference between a Navarro, Frenk, & White (1997, hereafter NFW) model and our best-fit profile. We calculated the fits, allowing correlations between these parameters, adjacent galaxies, and the main DM clumps. The largest extra mass that the model would support at any of these locations has a 1 σ upper limit of $2 \times 10^{11}\ h^{-1}\ M_\odot$.

The total mass profile is approximately represented by a single PL model with a central surface density $7900 \pm 100\ h\ M_\odot\ {\rm pc}^{-2}$, a $35 \pm 3\ h^{-1}$ kpc core, and a slope that is

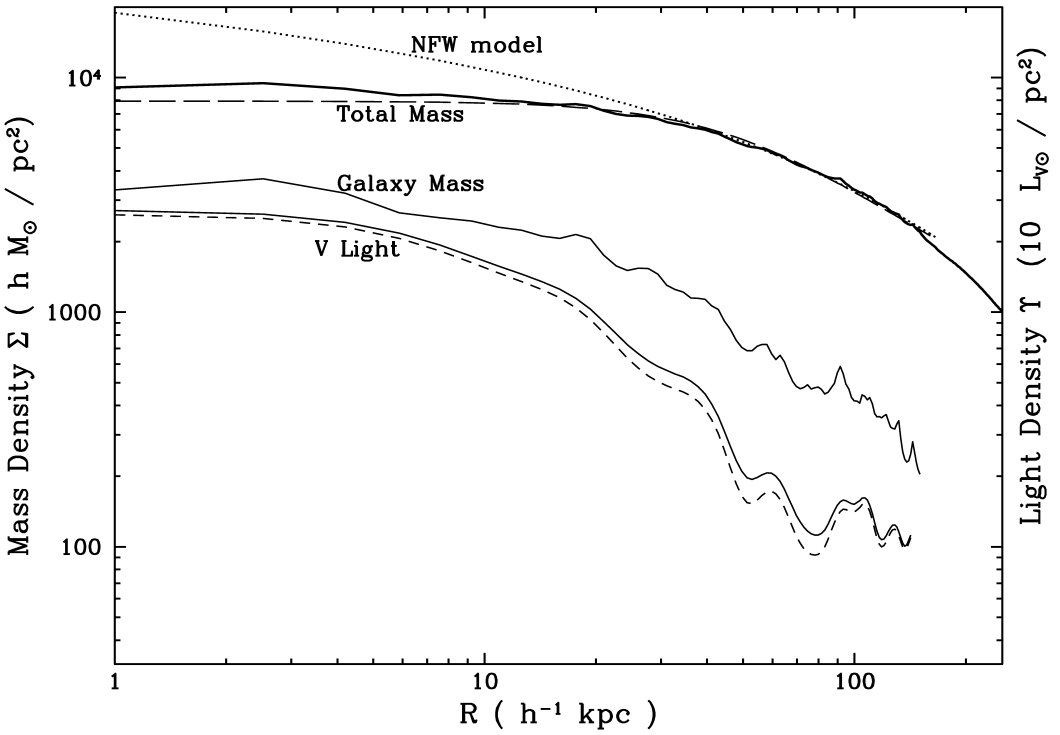

FIG. 4.—A radial plot of the mass density and light density. Total (*thick line*) and galaxy-only (*thin line*) components of the mass are shown. The dotted line is the best NFW fit discussed in the text, and the dashed line is the best-fit single PL model. The 35 h^{-1} kpc soft core in the mass is evident. A singular mass distribution is ruled out. The total rest-frame *V* light profile (*solid line*) and galaxy *V* light profile (*dashed line*), smoothed with a 5 h^{-1} kpc Gaussian, are also shown.

slightly shallower than an isothermal sphere ($\gamma = 0.57 \pm 0.02$). Outside the core, the model is indistinguishable from an NFW model mass distribution with $r_{200} = 2500\ h^{-1}$ kpc and concentration parameter $c = 8.05$. However, the presence of a soft core is in disagreement with the results from recent CDM simulations. For the NFW model that matches the mass distribution outside the core, the required mean mass density inside the inner (*E*) arc's radius is 40% (3500 $h\ M_\odot\ \mathrm{pc}^{-2}$) higher than observed (see Fig. 4). This corresponds to an extra interior mass of $2 \times 10^{12}\ h^{-1}\ M_\odot$, which we can rule out at greater than 10 σ: the position of arc *E* would be perturbed by over 20 pixels. Trading mass with the central galaxies also fails.

The total mass enclosed inside the 107 h^{-1} kpc radius of the arcs is

$$M_{107} = (1.662 \pm 0.002) \times 10^{14}\ h^{-1}\ d_{0.57}^{-1}\ M_\odot, \qquad (2)$$

where the dimensionless distance ratio $d_{0.57} = (D_{ls}/D_s)\,/0.57 = 1 \pm 0.15$ contains the uncertainty in the source redshift. The source's featureless spectrum, star-forming morphology and color, and presumed [O II] and Lyα emission lines suggest a redshift in the range $1.2 < z < 1.8$. Measures of mass segregation and clumpiness and the morphology are independent of $d_{0.57}$.

To allow a quantitative comparison of our results with future simulations, we have calculated a clumpiness measure for the projected mass density $\Sigma(\boldsymbol{r})$:

$$C^2 = A^{-1} \int_A \left[\frac{\Sigma(\boldsymbol{r}) - \Sigma(-\boldsymbol{r})}{\Sigma(\boldsymbol{r}) + \Sigma(-\boldsymbol{r})}\right]^2 d^2r, \qquad (3)$$

as an average of the normalized density asymmetry over the lens-plane area *A*, with $\boldsymbol{r}$ measured from the centroid that produces the smallest *C*. This measure is zero for twofold symmetric mass distributions, measures the deviation from smoothness, and is unaffected by ellipticity.

We calculate this statistic several ways: for mass not associated with luminous galaxies and for the total mass distribution, smoothed on three scales. All the *C* measures are integrated over a 107 h^{-1} kpc radius circle centered on the cluster DM [(1950) R.A. = $00^h23^m56\overset{s}{.}6$, decl. = 16°53′15″]. Using Gaussian smoothing with $\sigma = 10$, 20, and 40 h^{-1} kpc, we find $C = 0.071 \pm 0.005$, 0.049 ± 0.002, and 0.036 ± 0.001, respectively, for the full mass distribution. If we exclude the galaxies, $C = 0.025 \pm 0.003$, 0.029 ± 0.003, and 0.022 ± 0.002. The range of *C* includes uncertainties in the mass distribution, correction factors due to undersampling of the mass distribution, and a 10% variation in the radius of the circle of integration. This is a very smooth and symmetric distribution, even with the galaxies included, and the nongalaxy DM is smoother still. When comparing the results of *N*-body simulations with our data using equation (3), it is important that the simulations have both sufficient resolution and enough mass elements to ensure that the simulation's Poisson noise does not bias the statistic.

Wilson, Cole, & Frenk (1996) propose a mass quadrupole measure $Q(A)$, which may also distinguish between clusters in different cosmologies. For isodensity contours within 10% of $3820 d_{0.57}^{-1}\ h\ M_\odot\ \mathrm{pc}^{-2}$ (which has an area of $A = 1.2\ \mathrm{arcmin}^2$), we measure $Q(A) = 0.028 \pm 0.011$, for the total mass distribution. The largest part of the range comes from the choice of contour, because of the effect of cluster galaxies near the con-

tour. SCDM simulations typically give Q-values over 10 times larger than this.

We measure the diffuse intracluster light by fitting a four-parameter luminosity model to each of the 32 brightest galaxies, with the innermost 0.″5 of each excluded. A comparison between luminosity and mass profiles for galaxies will be given elsewhere (Dell'Antonio et al. 1998). The fit also includes a sky value and a seven-parameter elliptical PL model for the diffuse cluster light (I_0, $r_{\rm core}$, γ, x, y, $l_{\rm core}$, and θ). After subtracting the galaxy light, and excluding disks centered on fainter galaxies, we find that 15% ± 3% of the cluster light inside a 107 kpc radius is diffusely distributed. This diffuse light, shown in the bottom panel of Figure 3, has a core size of 7.″4, smaller than the DM core size, but the slopes of the distributions are nearly identical ($\gamma_{\rm light} = 0.49$). The center of the diffuse light is displaced only 3″ west-southwest from the DM center, and 7″ south-southwest from the total light centroid (which is centered on the large central ellipticals).

To examine the correlation between DM and stellar light, we require rest-frame photometry. The rest-frame V light is calculated from the observed F814 (791 nm) flux, since, for $z_{\rm cl} = 0.39$, the corresponding emitted wavelength is $791/(1 + z_{\rm cl}) = 569$ nm. Thus, the rest-frame absolute magnitude is

$$M_V = m_{\rm F814} + (M_V - M_{569}) - 25 - 5\log D_l - 2.5\log(1 + z_{\rm cl}) - 2.5\log(F^{\rm A}_{791}/F^{\rm A}_{569}), \quad (4)$$

where D_l is the luminosity distance and $F^{\rm A}$ is the flux of an A0 star. Taking $(M_V - M_{569}) = 0.05$ and $2.5\log(F^{\rm A}_{791}/F^{\rm A}_{569}) = 1.09$, $M_V = -39.83 + m_{\rm F814} + 5\log h$. Within a 107 h^{-1} kpc radius, the rest-frame V luminosity of the cluster is $(6.0 \pm 0.5) \times 10^{11}\ h^{-2}\ L_\odot$, yielding a global rest-frame mass-to-light ratio of $276 \pm 16 d_{0.57}^{-1}\ h\ (M/L_V)_\odot$. Because of luminosity evolution for $z > 0$ (Kelson et al. 1997), this is equivalent to a zero redshift $M/L_V = 390\ h\ d_{0.57}^{-1}\ (M/L_V)_\odot$.

In Figure 4, we plot the radially averaged mass and light profiles for CL 0024. The diffuse component of DM represents about 83% of the mass of the cluster inside 107 h^{-1} kpc, while the galaxies contribute the remaining 17%. Note that, averaged in this way, the M/L_V ratio increases 30%–40% from 20 to 100 h^{-1} kpc.

4. DISCUSSION

The mass distribution in CL 0024 is remarkably relaxed. If one assumes Gaussian density fluctuations in an $\Omega = 1$ universe, the fluctuation that seeded CL 0024 must have had a very large amplitude quite early (rare) in order to have become virialized by $z = 0.39$. One is led to consider non-Gaussian fluctuations or $\Omega \ll 1$. In the NFW hierarchical clustering model, our measured characteristic mass density $\delta_c = 2.6 \times 10^4$ implies (for $\Omega_0 = 0.3$) that the five largest progenitors contributed 50% or more of the cluster mass by a redshift of 2 (Navarro et al. 1997). More generally, these observations constrain any theory of structure formation on 300 kpc scales.

A key result of this first high-resolution mass map is the existence of a 35 h^{-1} kpc soft core. Any possible singularity must be quite small, contributing less than $2 \times 10^{11}\ h^{-1}\ M_\odot$ to the total mass within this core (10% of the mass of one of the central elliptical galaxies). Previous weak and strong lensing studies of clusters have found evidence for soft mass cores, more compact than the X-ray–derived cores (Tyson & Fischer 1995; Smail et al. 1996). Because cold collisionless particles have no characteristic length scale, the soft core suggests nongravitational interactions. While hot dark matter (HDM) can produce soft cores, HDM is not consistent with the high density of DM that we find in the individual cluster galaxies. Because of the relatively low X-ray luminosity ($0.7L^*_{\rm X}$), it is very unlikely that this can be attributed to hot gas alone. Galaxy halo stripping proceeds more rapidly at larger overdensities (Lokas et al. 1996), and the smaller core radius of the diffuse cluster light is consistent with some baryonic dissipation.

This first high-resolution mass map of a cluster of galaxies will be useful to compare with future N-body/gasdynamical simulations. None of the recent simulations show evidence of a soft core, in disagreement with these observations. Indeed, as the resolution of simulations increases from 100 to 30 kpc, the central mass becomes more singular. Higher resolution gasdynamical simulations for various initial fluctuation spectra and values of Ω will be required. Compared with current simulations, the smoothness of the DM distribution in CL 0024+1654 favors open, nonflat cosmologies. Constructing high-resolution mass maps of other clusters will require considerably deeper exposures, since we took advantage of an unusual, complex, high surface brightness galaxy directly behind the cluster.

REFERENCES

Colley, W. N., Tyson, J. A., & Turner, E. L. 1996, ApJ, 461, L83
Crone, M. M., Evrard, A. E., & Richstone, D. O. 1994, ApJ, 434, 402
———. 1996, ApJ, 467, 489
Dell'Antonio, I. P., Kochanski, G. P., & Tyson, J. A. 1998, in preparation
Dressler, A., & Gunn, J. E. 1992, ApJS, 78, 1
Efron, B. 1982, The Jackknife, the Bootstrap, and Other Resampling Plans (Philadelphia: SIAM)
Eke, V. R., Cole, S., & Frenk, C. S. 1996, MNRAS, 282, 263
Evrard, A. E., Mohr, J. J., Fabricant, D. G., & Geller, M. J. 1993, ApJ, 419, L12
Frenk, C. S., Evrard, A. E., White, S. D. M., & Summers, F. J. 1996, ApJ, 472, 460
Jing, Y. P., Mo, H. J., & Fang, L. Z. 1995, MNRAS, 276, 417
Kelson, D. D., et al. 1997, ApJ, 478, L13
Kochanski, G. P., Tyson, J. A., & Dell'Antonio, I. P. 1998, in preparation
Lokas, E. L., Juszkiewicz, R., Bouchet, F. R., & Hivon, E. 1996, ApJ, 467, 1
Mohr, J. J., Evrard, A. E., Fabricant, D. G., & Geller, M. J. 1995, ApJ, 447, 8
Moore, B., Ghigna, S., Governato, F., Lake, G., Quinn, T., & Stadel, J. 1997, preprint (astro-ph/9711259)
Navarro, J. F., Frenk, C. S., & White, S. D. M. 1997, ApJ, 490, 493
Ostriker, J. P., & Cen, R. 1996, ApJ, 464, 270
Schindler, S., & Böhringer, H. 1993, A&A, 269, 83
Schneider, P., Ehlers, J., & Falco, E. E., 1993, Gravitational Lenses (New York: Springer)
Schramm, T. 1994, A&A, 284, 44
Smail, I., et al. 1996, ApJ, 469, 508
———. 1997, ApJ, 479, 70
Thomas, P.A., et al. 1997, MNRAS, submitted (astro-ph/9707018)
Tyson, J. A., & Fischer, P. 1995, ApJ, 446, L55
Tyson, J. A., Kochanski, G. P., & Dell'Antonio, I. P. 1997, in The UV Universe at Low and High Redshift, ed. W. Waller, M. Fanelli, J. Hollis, & A. Danks (New York: AIP), 207
Wilson, G., Cole, S., & Frenk, C. S. 1996, MNRAS, 282, 501

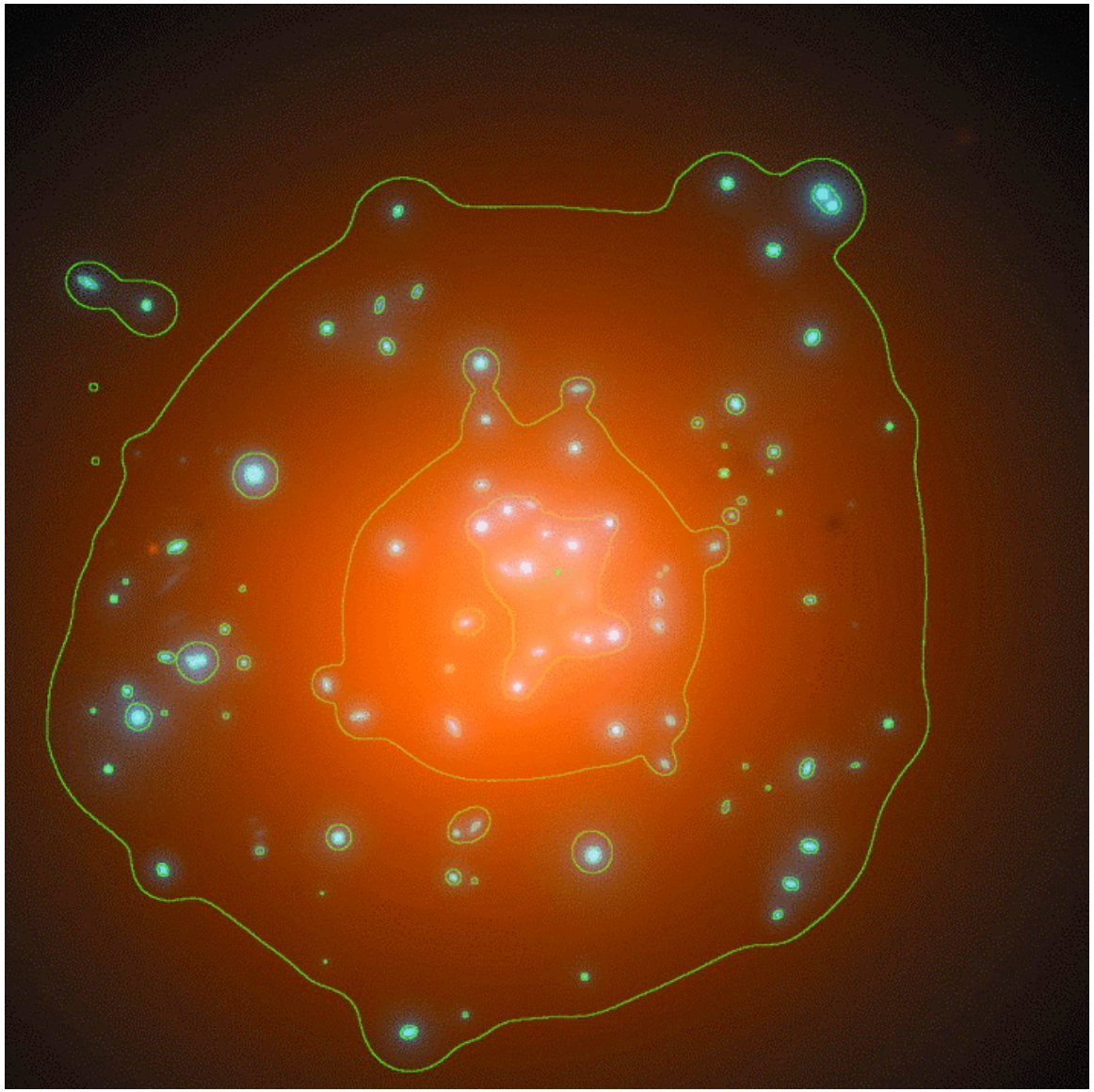

Fig. 1.— The reconstructed total mass density in CL 0024 is shown as a color-coded mass image. The DM is shown in orange. The mass associated with visible galaxies is shown in blue. The contours are at 0.5, 1, and 1.5 times the critical lensing density (4497 $h\,d^{-1}_{0.57}\,M_{\odot }$ pc $^{-2}$), with heavier contour at the critical lensing density. This image is 336 h^{-1} kpc across. North is up, and east is left.

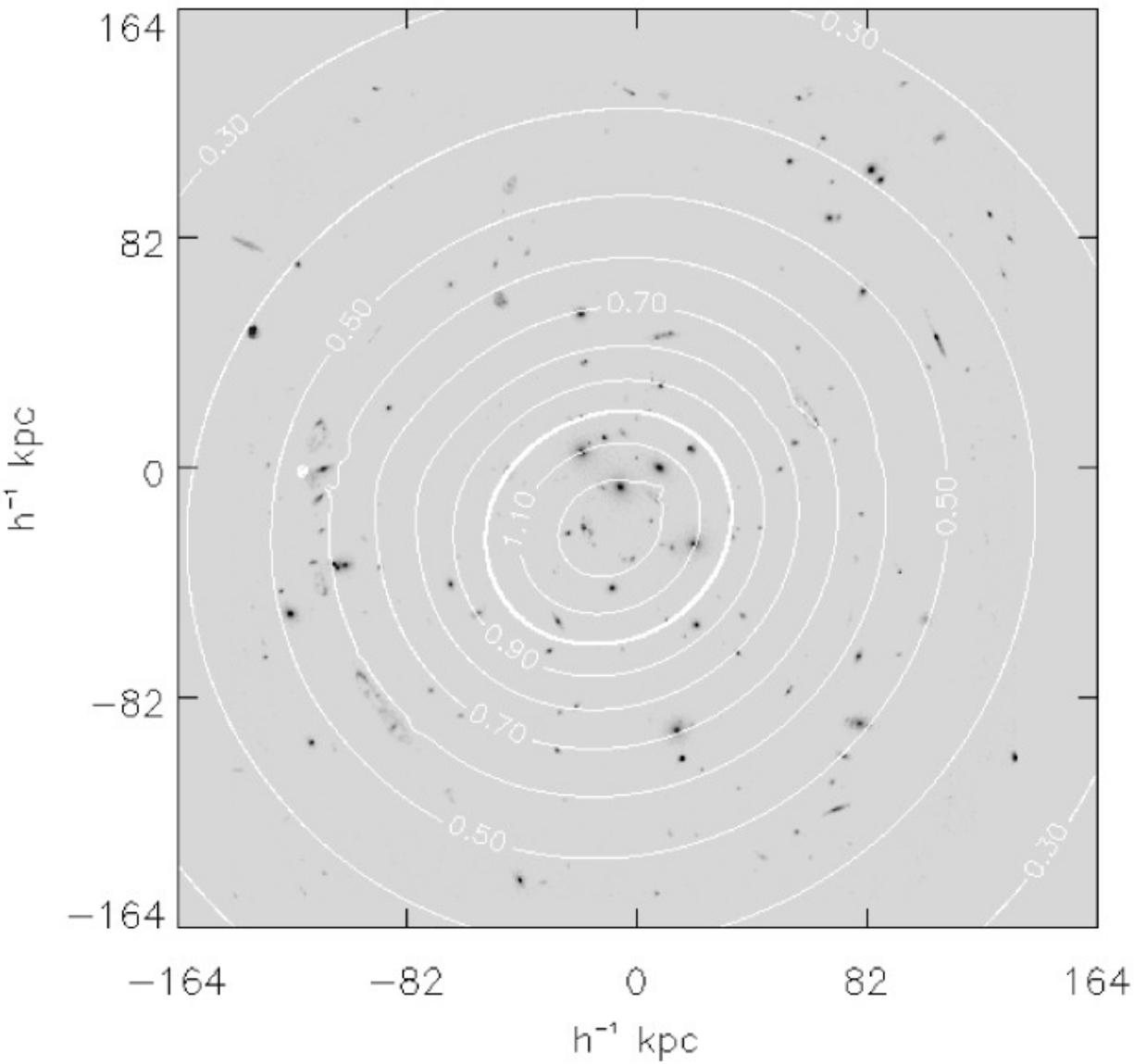

Fig. 2.— The reconstructed mass density not associated with visible galaxies in CL 0024 is shown as a contour plot (white contours), superposed on the F450W (blue) HST image for reference. Isomass contours for this dark mass are at $0.1\Sigma _{c}$ intervals in projected mass density, with a thick contour at 1 $\Sigma _{c}$, as labeled. The plot is $336\,h^{-1}$ kpc (100 $\arcsec$) across, centered at R.A. = 00h23m56 $\fs$ 6, decl. = 16°53 $\arcmin$ 15 $\arcsec$ (1950). On scales larger than 10 kpc, this majority component of the DM is remarkably smooth. The DM substructure has already been erased by $z=0.39$.

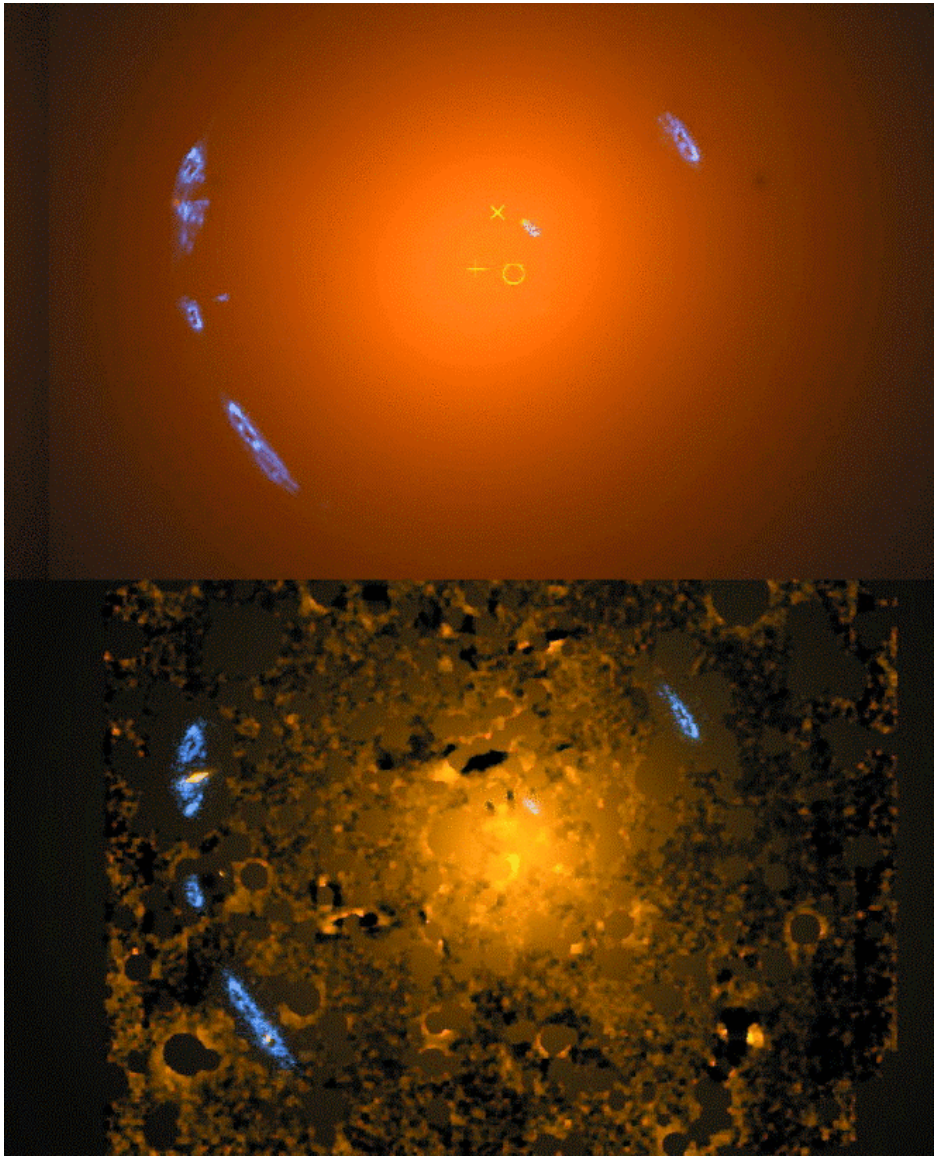

Fig. 3.—Top panel: the cluster mass density not associated with galaxies is shown in orange. The centers of the DM (plus sign), total light (cross), and diffuse light (circle) distributions are marked. The reconstructed optical arcs are shown superposed in blue. Bottom panel: the diffuse light component of the cluster is shown in orange. Galaxies have been fitted and subtracted, and their cores are replaced with the fit to the diffuse light. The HST images of the arcs are then superposed in color (one blue and two yellow galaxies projected on the arcs are reinserted here but are not counted in the diffuse light). Note the excellent agreement of the modeled arcs (top panel) and the data (bottom panel). The demagnified source image just west of the center strongly constrains the mass profile in the core.